OPEN ACCESS Freely available online

ISSN: 2157-7463
Journal of Petroleum & Environmental Biotechnology

Review article

Evaluation of Sedimentary Basins for Hydrocarbon Exploration Using Aeromagnetic Data, Northwestern Sinai Peninsula, Egypt

Gaber M. Gaber*

Department of Geology, Helwan University, Cairo, Egypt

ABSTRACT

The Sinai Peninsula's northwestern area has many structure patterns with different directions and strong variations in basement depth. This work aims to deduce the basement surface's depth and sedimentary basin's locations and evaluate the subsurface structural framework to determine the new concession for hydrocarbon exploration in the research area.

Geophysical data used in this study compiled between total aeromagnetic intensity (TM) data and wells data as locations and depths were used in 2D magnetic profiles in basement depth determination. The technique used for magnetic data interpretation to determine basement depth and structures include; Reducing to the Pole (RTP), power spectrum (low and high pass filters to determine deep and shallow sources), and Centre for Exploration Targeting (CET) grid analysis.

Therefore, according to these results, the basement depths range from 1500 to 5000 meters and the area has two principal structural trends: NW-SE trends related to extensions that happened in the Delta belt (Hing line) north Pelusium line and NE-SW trends associated with the Syrian arch system compressional force south Pelusium line. The new concession for hydrocarbon exploration is represented in the northwestern part of the study area.

Keywords: 2D modelling; Basement relief; Aeromagnetic data; Structure framework; CET technique

INTRODUCTION

The study area is located between Long (32° 30'-33° 30') and Lat (30° 20' -31° 10') in the Northwestern part of the Sinai sub-plate (Figure 1). It includes oil prospects in the north, coal at Gebel el Moghara and soil water potentials in the east and south portions of the study area, and it has significant economic importance.

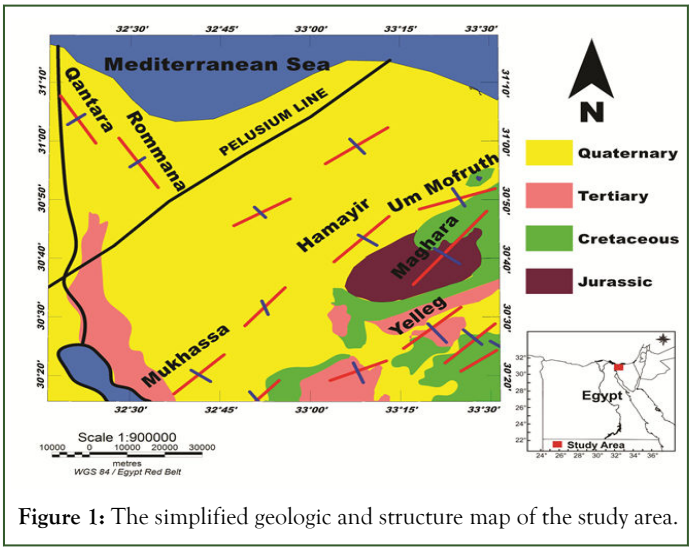

Figure 1: The simplified geologic and structure map of the study area.

Correspondence to: Gaber M. Gaber, Department of Geology, Helwan University, Cairo, Egypt; E-mail: Gaber.magdy@science.helwan.edu.eg

Received: 05-Aug-2023, Manuscript No. JPEB-23-22698; **Editor assigned:** 08-Aug-2023, PreQC No. JPEB-23-22698 (PQ); **Reviewed:** 23-Aug-2023, QC No. JPEB-23-22698; **Revised:** 09-Jan-2025, Manuscript No. JPEB-23-22698 (R); **Published:** 16-Jan-2025, DOI: 10.35248/2157-7463.24.16.594

Citation: Gaber MG (2025) Evaluation of Sedimentary Basins for Hydrocarbon Exploration Using Aeromagnetic Data, Northwestern Sinai Peninsula, Egypt. J Pet Environ Biotechnol. 16:594.

The magnetic data is used to define the contacts between various rocks that generally occur along the fault lines. The magnetic anomalies map clarifies faults affecting basement lithology that may control the sedimentary basins evolutions and depositional history in petroleum exploration. The interpretation of the magnetic anomalies map reflect the subsurface geologic conditions in the area under investigation [1].

This work aims to understand the regional subsurface structural framework and deduce the basement surface depth in the research area in two steps (analyzing and interpreting) the magnetic data. Finally determined the best location for hydrocarbon exploration in the study area.

Geologic and tectonic settings

The numerous marine transgressions came from N to NW and covered Egypt's the Sinai Peninsula and several other basins. This area is characterised by different ages of rock units ranging from older to younger ages (Triassic, Jurassic, Cretaceous, Tertiary and Quaternary) (Figure 2). The most common events in the study area during the Cretaceous and Eocene ages (e.g. as existed in South Yalleg basins and Central Sinai) reached the Jurassic (e.g., East Maghara, North Maghara), the Triassic and the Carboniferous rock units [2].

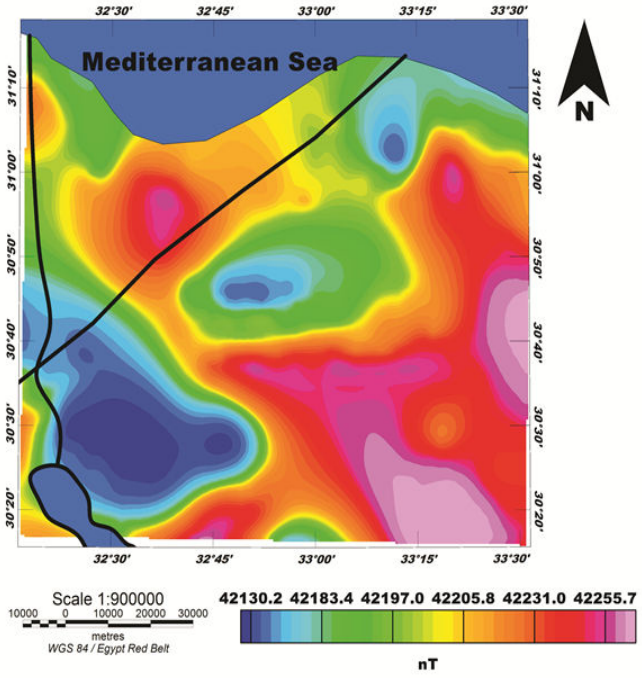

Figure 2: Total intensity aeromagnetic map of the study area.

The Northwestern part of Sinai is characterised as featureless as the south part of the Pelusium line in which the outcropped Maghara Mountain was an elevated area with trending NE–SW. The southern part of the Pelusium line is also characterised by several NE-SW trending anticlines such as Gabal Yelleg, with elongated synclines in between.

The Northwestern Sinai area is characterised by structures extending from Jordan and Syria in the east to the Western Desert in the west, following the Syrian Arc as (Mesozoic faulted domes, anticlines, and synclines). The Northwestern part of Sinai has the regional mega shear as the oldest structural trend in the NNE–SSW shear zone trend known as the Pelusium line. Before bending to the north, the eastern extension of the Pelusium line cuts across the Norte Sinai Continental Shelf, creating a sequence of SSW NNE striking faults that follow the Palestinian continental slope. Meshref, Meshref and Hammouda and Gaber et al., reported that the Sinai Peninsula was subdivided into different basins and different tectonic blocks. The most northern blocks south of the Pelusium line are divided into two sub-blocks by the Mesozoic hinge line. The northern sub-block is mainly characterised by thrusting and folding. Besides, at least from the time of Oligo–Miocene, tensional forces seem to affect the southern subblock and are characterised by NW-SE normal fault trend relative to the Suez Gulf rift and NNE-SSE trend near the Gulf of Aqaba [3].

The northwestern extensional basins in the north Pelusium line (as Qantara and Rommana) are related to The Hinge Zone (Nile Delta Faulted Flexure Zone). During the Jurassic-Cretaceous time, this area includes a major structural element related to the southern Neo-Tethys crustal breakup. It contains roughly E-W oriented, arced and narrow zones of normal faults in North Sinai and Palestine that formed a westward continuation.

LITERATURE REVIEW

Data

The total intensity magnetic anomaly map (TM) of the studied area is compiled with a scale of 1:500,000 and a 5nT contour interval by Ismail et al. (Egyptian Geological Survey and Mining Authority (EGSMA). The measured magnetic data were corrected to the base station of continuous recording to reduce the earth's magnetic field variation. IGRF (international geomagnetic reference field) was calculated for the measuring stations. The measured data were tied to a single base station at Abu Zenema with latitude 29° 04'N and longitude 33° 11'E. The total intensity magnetic field in nT was measured with a proton precession magnetometer model G-816, as a field instrument with an accuracy of 1 nT. Diurnal variations of the earth's magnetic field were measured by continuous recording at the base station with a 1 minute time interval to observe the earth's diurnal activity. The stationary base station instrument is an ENVI MAG magnetometer with 0.1 nT accuracies [4].

Geophysical data analysis

Aeromagnetic data is one process that simplifies aeromagnetic data analysis depending on source magnetization. The Reduced to the Pole (RTP) filter is applied to (TM) with magnetic parameters inclination 44.2° and declination 2.2°. This step is for data preparation to power-spectrum separation [5].

The aeromagnetic map (Figure 3) illustrates that magnetization values range from 42105.7 nT to 42280.3 nT. The magnetic anomalies are elongated and arranged along E-W, NW-SE, and NE-SW trends [6]. The southeastern part of the research area has a high magnetic anomaly and the area is affected by the Syrian arch system compressional force where the area is

elevated and has some mountains. The northwestern study area has low magnetization because basins characterize this area's Hing line extensional event in the Delta belt [7].

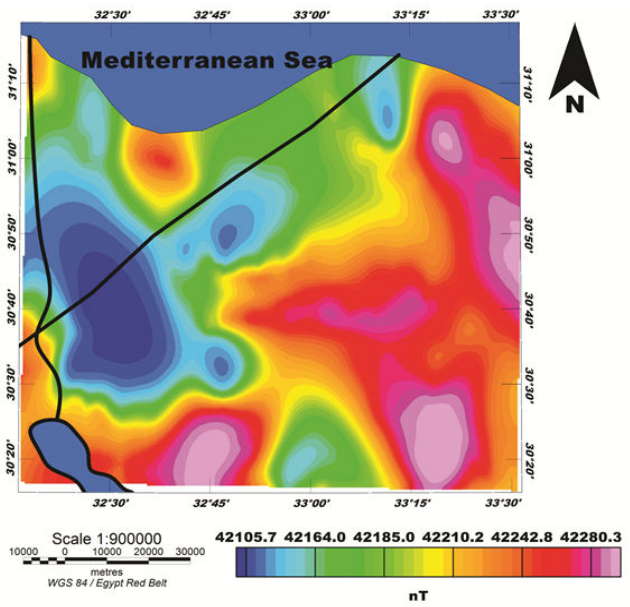

Figure 3: RTP aeromagnetic map of the study area.

The regional and residual separation are applied on the RTP map (Figure 4) to separate deep and shallow magnetization sources. This filter is separated on power-spectrum at value 0.025 cycle/km (Figure 5).

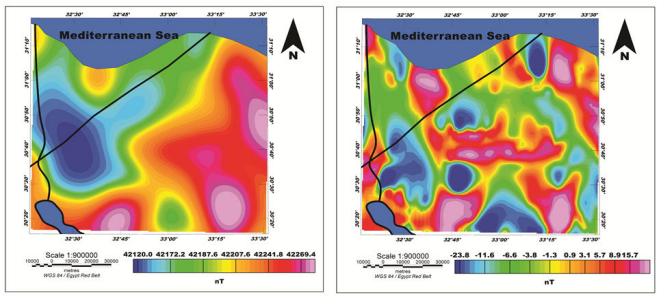

Figure 4: (A) Regional, (B) Residual aeromagnetic maps of the study area.

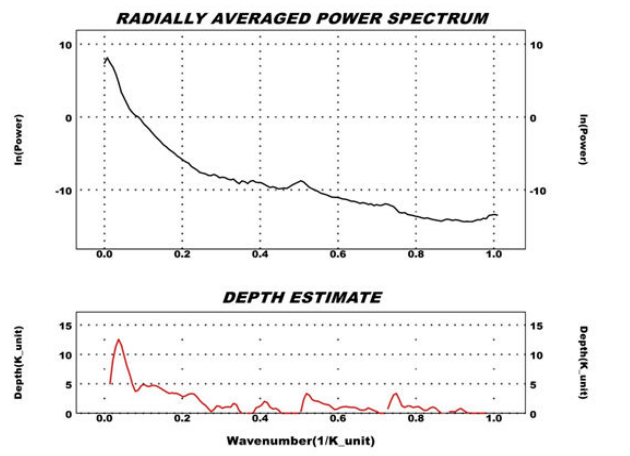

Figure 5: Radially average power-spectrum of RTP data.

The regional map illustrated the shape of the basement surface, which is shallower in the southeastern part of the research area and deeper in the northwestern part and ranged from 42120 nT to 42269.4 nT. Furthermore, Figure 4B showed the study area's residual map, referred to as shallow magnetization sources of the study area, and ranged in its values from -23.8 nT to 15.7 nT [8].

Edge detecting by Centre for Exploration Targeting (CET) grid analysis

The CET grid analysis system analyses an image's texture to detect structural complexity areas in the study area. The deposit occurrence is located by using structural complexity analysis. This method identifies magnetic discontinuities utilizing a combination of texture analysis and bilateral symmetric feature detection. Figure 6 shows the lineaments map extracted from the CET grid analysis technique.

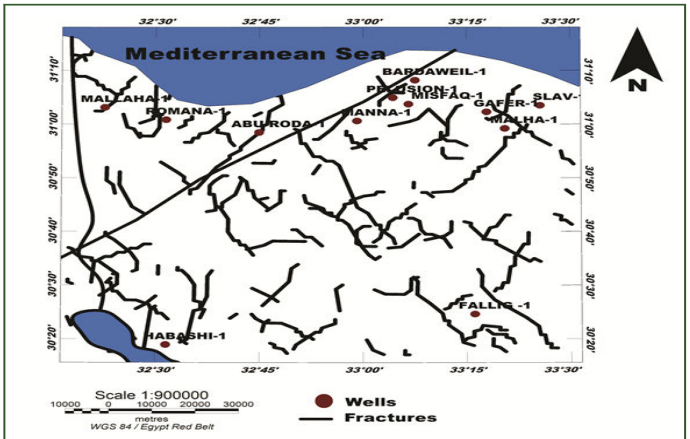

Figure 6: Centre for Exploration Targeting (CET) Grid analysis map.

2D magnetic modelling

Instead of modelling each data individually, the sequence of the original magnetic data resulted in limited interpretation results. Among magnetic data, the physical property used in modelling was the susceptibility of rocks. The 2D magnetic profiles were constructed from Aeromagnetic data integrated with wells data along the study area. Three 2D profiles (M1, M2, M3) (Figure 7) were constructed over the study area in the directions E-W, NW-SE, and NE-SW to determine basement surface depths and the wells data used in these models are mentioned in Table 1.

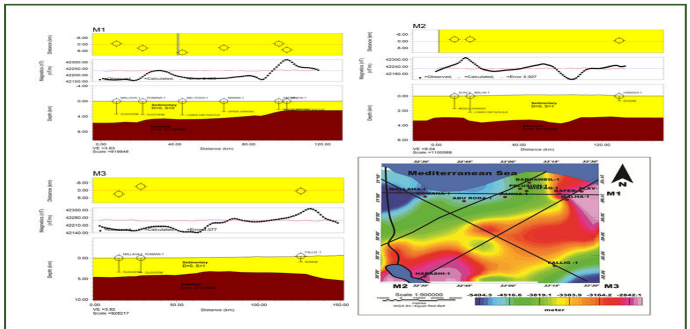

Figure 7: (A) Profile M1 (B) Profile M2 (C) Profile M3 and (D) Basement surface depth map extracted from profiles with profile locations.

Table 1: The wells data used in 2D magnetic profiles.

WELL	LONG	LAT	FTD (m)	FMTD	Company
Mallaha-1	32.37722	31.05208	3371.088	Oligocene	Gulf oil
Romana-1	32.52497	31.01406	3505.2	Oligocene	Gulf oil
Manna-1	32.98556	31.01056	2702.357	Upper Jurassic	Israel
Pelusion-1	33.07194	31.08278	2499.055	Oligocene	Israel
Misfaq-1	33.10975	31.06267	3169.92	Cretaceous	I.E.O.C.
Gafer-1	33.29806	31.03833	2157.07	Middle Jurassic	Israel
Slav-1	33.42722	31.05833	1698.65	Middle Jurassic	Israel
Abu roda-1	32.74922	30.97475	3619.5	Lower cretaceous	CONOCO
Malha-1	33.342	30.98686	2198.218	Lower cretaceous	I.E.O.C.
Bardaweil-1	33.12542	31.13694	4114.8	Jurassic	I.E.O.C.
Fallig-1	33.26867	30.41053	1371.6	Shusha	GUPCO
Habashi-1	32.525	30.31583	658.368	Eocene	A.E.O.

Figure 7 shows the basement surface depth map extracted from 2D magnetic modelling along the study area with three models and wells location.

RESULTS AND DISCUSSION

According to the Edge detecting technique (CET), the study area's structural evaluation gives two principal trends (NE-SW and NW-SE). The research area is divided into two parts by the Pelusium line. The southeastern part was exposed to compressional force and Africa moved west-northwest relative to Eurasia during the Late Cretaceous to early tertiary time, which closed the Tethys Sea and produced a right-lateral shear couple between North Africa and Eurasia. The asymmetrical NE-SW trend produced by the tectonic event is known in the Middle East as the Syrian arc system. The fractures in the direction NW-SE are related to this event, and the compressional force should be affected by basement depth, so this area is characterized by high mountains. Figures 6 illustrated the directions of this area south of the Pelusium line.

The northwestern part, which is part of the Delta belt and this area is characterized by extensional force in the direction NW-SE during the Jurassic-Cretaceous time and produced fractures in the direction NE-SW, and basins characterize these fractures related to the Hing Line fault zone and this area as (Qantara and Rommana) and basement depth in this area is increased. Figures 6 show the direction of the north of the Pelusium line.

Furthermore, the basement depth map extracted from 2D magnetic models (Figure 7) is ranged from 2000 to 5500 meters, and this result is suitable with previous work such as Gaber et al.

The Regional map of the Aeromagnetic map has described the basement as being elevated in the southeastern part while the northwestern region is depressed.

Finally, according to the results of edge detecting and basement surface depth techniques (Figures 7 and 8) the research area is divided into two principal parts. The northwestern part has basins, and the basement surface is deep and reached 5000 meters the structure trends in the direction of NE-SW are related to the Hige line of the Delta belt. Secondly, the southeastern part is elevated in the basement surface and characterized by structural trends related to the Syrian arch system movement in the NW-SE direction.

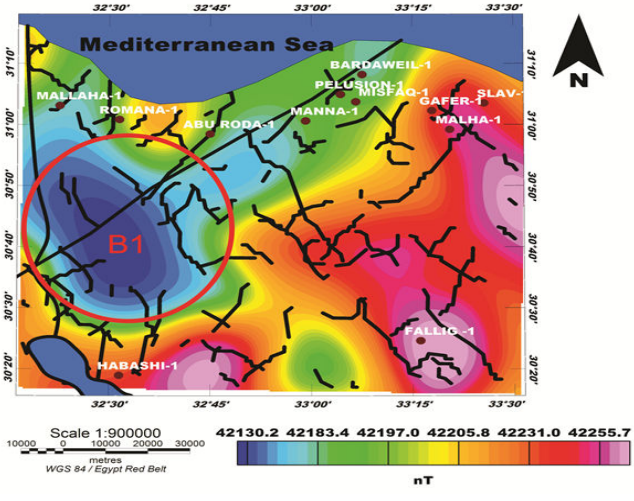

Figure 8: Decision map for best hydrocarbon new concession.

Figure 8 shows the combined map between the regional magnetic map that represents the large basin in the west area this basin has more limitations or structures so can say this basin B1 is suitable for hydrocarbon exploration studies.

CONCLUSION

The obtained result from different techniques in this work in structure evaluation or basement detecting. The basement depth is ranged along the study area from 1500 to 5000 meters, the southeastern is elevated and the northwestern part is characterized by basins. The northwestern part is characterized by a large basin called B1. This basin is suitable for more exploration studies and according to this evaluation, this area is a promising area for large hydrocarbon reservation.

DATA AVAILABILITY

The data that support the findings of this study are available from the corresponding author upon reasonable request.

CONFLICT OF INTEREST

I confirmed that there are no known conflicts of interest associated with this publication, and there has been no significant financial support for this work that could have influenced its outcome.

REFERENCES

1. Montiel C, Quintero R, Aburto J. Petroleum biotechnology: technology trends for the future. African J Biotechnol. 2009;8(12).
2. Quijano G, Hernandez M, Thalasso F, Munoz R, Villaverde S. Two-phase partitioning bioreactors in environmental biotechnology. Appl Microbiol Biotechnol. 2009;84:829-846.
3. Mahjoubi M, Jaouani A, Guesmi A, Amor SB, Jouini A, Cherif H, et al. Hydrocarbonoclastic bacteria isolated from petroleum contaminated sites in Tunisia: isolation, identification and characterization of the biotechnological potential. New Biotechnol. 2013;30(6):723-733.
4. El-Naas MH, Alhaija MA, Al-Zuhair S. Evaluation of a three-step process for the treatment of petroleum refinery wastewater. J Environ Chem Engin. 2014;2(1):56-62.
5. Miri S, Naghdi M, Rouissi T, Kaur Brar S, Martel R. Recent biotechnological advances in petroleum hydrocarbons degradation under cold climate conditions: A review. Critical Reviews Environ Sci Technol. 2019;49(7):553-586.
6. Zhang Z, Gai L, Hou Z, Yang C, Ma C, Wang Z, et al. Characterization and biotechnological potential of petroleum-degrading bacteria isolated from oil-contaminated soils. Bioresource Technol. 2010;101(21):8452-8456.
7. Daâssi D, Qabil Almaghribi F. Petroleum-contaminated soil: environmental occurrence and remediation strategies. Biotech. 2022;12(6):139.
8. Le Borgne S, Quintero R. Biotechnological processes for the refining of petroleum. Fuel Processing Technol. 2003;81(2): 155-169.